pH stability of the Stromelysin-1 Catalytic Domain and its mechanism of interaction with a glyoxal inhibitor

Nicole Howe[a,b], Mariangela Ceruso[a,b], Edward Spink[a], and J.Paul.G. Malthouse[a]*

[a] UCD School of Biomolecular and Biomedical Science, UCD Centre for Synthesis and Chemical Biology, SEC Strategic Research Cluster, Conway Institute, University College Dublin, Belfield, Dublin 4, Ireland.

[b]These authors made equally important contributions to this work.

*Corresponding author. UCD School of Biomolecular and Biomedical Science, UCD Centre for Synthesis and Chemical Biology, SEC Strategic Research Cluster, Conway Institute, University College Dublin, Dublin 4, Ireland. Tel.: 0035317166872; Fax 0035317166893

E-mail address: J.Paul.G.Malthouse@ucd.ie (J.P.G. Malthouse)

ABSTRACT

The Stromelysin-1 catalytic domain$^{83-247}$ (SCD) is stable for at least 16 hours at pHs 6.0-8.4. At pHs 5.0 and 9.0 there is exponential irreversible denaturation with half lives of 38 and 68 min respectively. At pHs 4.5 and 10.0 irreversible denaturation is biphasic. At 25°C, C-terminal truncation of stromelysin-1 decreases the stability of the stromelysin-1 catalytic domain at pH values > 8.4 and < 6.0. We describe the conversion of the carboxylate group of (β*R*)-β-[[[(1*S*)-1-[[[(1*S*)-2-Methoxy-1-phenylethyl]amino]carbonyl]-2,2-dimethylpropyl]amino]carbonyl]-2-methyl-[1,1'-biphenyl]-4-hexanoic acid (UK-370106-COOH) a potent inhibitor of the metalloprotease stromelysin-1 to a glyoxal group (UK-370106-CO^{13}CHO). At pH 5.5 - 6.5 the glyoxal inhibitor is a potent inhibitor of stromelysin-1 (K_i = ~1 μM). The aldehyde carbon of the glyoxal inhibitor was enriched with carbon-13 and using Carbon-13 NMR we show that the glyoxal aldehyde carbon is fully hydrated when it is in aqueous solutions (90.4 ppm) and also when it is bound to SCD (~92.0 ppm). We conclude that the hemiacetal hydroxyl groups of the glyoxal inhibitor are not ionised when the glyoxal inhibitor is bound to SCD. The free enzyme pK_a values associated with inhibitor binding were 5.9 and 6.2. The formation and breakdown of the signal at ~92 ppm due to the bound UK-370106-CO^{13}CHO inhibitor depends on pK_a values of 5.8 and 7.8 respectively. No strong hydrogen bonds are present in free SCD or in SCD-inhibitor complexes. We conclude that the inhibitor glyoxal group is not directly coordinated to the catalytic zinc atom of SCD.

Keywords

pKa, metalloprotease, tetrahedral intermediate, glyoxal inhibitor, pH stability

Abbreviations: UK-370106-COOH, (β*R*)-β-[[[(1*S*)-1-[[[(1*S*)-2-Methoxy-1-phenylethyl]amino]carbonyl]-2,2-dimethylpropyl]amino]carbonyl]-2-methyl-[1,1'-biphenyl]-4-hexanoic acid,; ZBG, zinc-binding group;SCD, stromelysin-1 catalytic domain$^{83-247}$; MCA, (7-methoxycoumarin-4-yl)acetyl; Dnp, 2,4 dinitrophenyl.

1. Introduction

Specific peptide-derived glyoxal inhibitors have been shown to be potent inhibitors of the serine proteases [1-5], the cysteine proteases [5-8] and the aspartyl proteases [9, 10]. Glyoxal inhibitors are most effective with the cysteine proteases and their active site thiol group has been shown to form a thiohemiacetal with the glyoxal aldehyde group [6]. The aspartyl proteases bind the fully hydrated glyoxal, which mimics the tetrahedral intermediate thought to be formed during catalysis [9]. In the serine proteases the active site serine hydroxyl group has been shown to form a hemiketal with the keto-carbon of the glyoxal group, this hemiketal mimics the tetrahedral intermediate formed during catalysis [1, 2, 11]. In serine protease-glyoxal inhibitor complexes it has been shown that the pK_a values of both the glyoxal hemiketal and hemiacetal hydroxyl groups have been reduced by 5-7 pK_a units [1, 3]. The primary cause of the reductions in the pK_a values of the hydroxyl-groups is thought to be due to the presence of the positively charged active site histidine [1, 3, 4, 12].

In the metalloproteases an active site zinc atom is thought to play a similar role by lowering the pK_a of the hydroxyl groups of a bound water molecule and by stabilizing the oxyanion of the catalytic tetrahedral intermediate [13-15]. As both the keto and aldehyde groups of the glyoxal group of peptide glyoxals are readily hydrated [1, 11] we expected that the hydroxyl groups of the hydrated glyoxal would be coordinated to the active site zinc atom of a metalloprotease such as stromelysin-1 (E.C. 3.4.24.17). This coordination to the positively charged zinc atom should lower the pK_a values of the hydroxyl groups of the hydrated glyoxal promoting the coordination of the oxyanion to the catalytic zinc and allowing the glyoxal group to function as an effective zinc binding group (ZBG).

Metalloprotease inhibitors can be classified as being designed to bind in the left hand side (P_3-P_2-P_1-ZBG) or the right hand side (ZBG-P_1'-P_2'-P_3') of the active site or on both sides (P_3-P_2-P_1-ZBG-P_1'-P_2'-P_3'). Inhibitors binding on the right hand side of the active site are usually the most potent metalloprotease inhibitors [16]. Chemists at Pfizer have synthesized (β*R*)-β- [[[(1*S*)-1-[[[(1*S*)-2-Methoxy-1 phenylethyl]amino]carbonyl]-2,2 dimethylpropyl]amino]carbonyl]-2-methyl-[1,1'-biphenyl]-4-hexanoic acid (UK-370106-COOH) (Scheme 1) a potent right hand side inhibitor of the

metalloprotease stromelysin-1 with a carboxylate zinc-binding group [17, 18]. We have converted the carboxyl zinc binding group of this inhibitor to a glyoxal group with ^{13}C-enrichment in the glyoxal aldehyde carbon (UK-370106-CO^{13}CHO). This allows us to use ^{13}C-NMR to determine whether there is oxyanion stabilisation within the stromelysin-1-UK-370106-CO^{13}CHO inhibitor complexes and ^{1}H-NMR to determine if there are any low barrier hydrogen bonds present. Our catalytic and NMR studies at different pHs require that stromelysin-1 be stable during data acquisition. Therefore we have undertaken a study of the pH stability of stromelysin-1 to ensure that there is no significant irreversible denaturation during our experiments. In order to facilitate our NMR studies all this work has been carried out using the stromelysin-1 catalytic domain containing residues 83-247.

The stromelysins are metalloproteases which include stromelysin-1 (MMP-3), stromelysin-2 (MMP-10) and stromelysin-3 (MMP-11). Matrilysin (MMP-7) is closely related to the stromelysin-1 but it lacks its C-terminal domain and so it is similar to the C-terminal truncated stromelysin-1 (residues 83-247) examined in the present work [16]. As all these metalloproteases have similar active sites we would expect their catalytic domains to undergo similar interactions with glyoxal inhibitors. Therefore our studies with the stromelysin-1 catalytic domain (residues 83-247) should provide important insights into how glyoxal inhibitors interact with the stromelysins and similar metalloproteases such as matrilysin. However, with less closely related metalloproteases there may be significant differences in their interactions with glyoxal inhibitors.

2. Materials and methods

2.1.Materials

The inhibitor UK-370106-COOH ((β*R*)-β-[[[(1*S*)-1-[[[(1*S*)-2-Methoxy-1 phenylethyl]amino]carbonyl]-2,2-dimethylpropyl]amino]carbonyl]-2-methyl-[1,1'-biphenyl]-4-hexanoic acid) was obtained from Tocris Bioscience, Tocris House, IO Centre, Moorend Farm Avenue, Avonmouth, Bristol BS11 0QL, UK. The fluorescence substrate (7-methoxycoumarin-4-yl)acetyl-L-arginyl-L-prolyl-L-lysyl-L-prolyl-L-valyl-L-glutamyl-L-norvalyl-L-tryptophyl-L-

arginyl-N^e-(2,4-dinitrophenyl)-L-lysine amide was obtained from Peptanova Gmbh, Keplerstr. 26, 69207 Sandhausen, Germany. The thiopeptolide substrate Acetyl-Proline-Leucine-Glycine-[2-mercapto-4-methyl-pentanoyl]-Leucine-Glycine-OC_2H_5 was obtained from Enzo Life Sciences (UK) Ltd., Palatine House, Matford Court, Exeter EX2 8NL, UK. The Macro-Prep High Q Support anion exchange column was obtained from Bio-Rad Laboratories, Inc. Life Science Group 2000 Alfred Nobel Drive, Hercules, CA 94547, USA. A pET3a plasmid containing the recombinant stromelysin-1 catalytic domain (SCD) containing residues 83-247 was a generous gift from Professor Hideaki Nagase. All other materials were obtained from Sigma-Aldrich Chemical Co., Gillingham, Dorset, U.K.

2.2. NMR spectra of the (3R)-3-{(1S)-1-[(1S)-2-Methoxy-1-phenyl-1-ethyl]carbamoyl-2, 2-dimethyl-1-propyl}carbamoyl-6-(2-methyl-1, 1'-biphenyl-4-yl) Hexanoic Acid (UK-370106-COOH) inhibitor

The ^{1}H-NMR and ^{13}C-NMR spectra of this compound at 400 MHz have been reported but only the ^{1}H-NMR spectrum was partially assigned at 400MHz [17]. We have fully assigned both the ^{1}H-NMR and the ^{13}C-NMR spectrum at 500 MHz. ^{1}H NMR (500 MHz, [^{2}H]chloroform) δ 1.04 (9H, s, $CHC(CH_3)_3$), 1.32-1.71 (4H, m, $CH_2CH_2CH_2C_6H_5$), 2.20 (3H, s, $C_6H_5CH_3$), 2.33-2.81 (5H, m, $HOOCCH_2CH$ and $CH_2CH_2CH_2C_6H_5$), 3.36 (3H, s, CH_2OCH_3), 3.61-3.70 (2H, m, CH_2OCH_3), 4.55 (1H, d, J=9.7 Hz, $CHC(CH_3)_3$), 5.15-5.23 (1H, m, $C_6H_5CHCH_2OCH_3$), 6.8-7.44 (15H, m, $2C_6H_5$, C_6H_3, 2NH). ^{13}C-NMR ([^{2}H] chloroform) δ = 20.43 (1C, $C_6H_5CH_3$), 26.62 (3C, $CHC(CH_3)_3$), 28.76 (1C, $CH_2CH_2CH_2C_6H_5$), 32.28 (1C, $CH_2CH_2CH_2C_6H_5$), 34.76 (1C, $CHC(CH_3)_3$), 35.19 (1C, $CH_2CH_2CH_2C_6H_5$), 36.62 (1C, $HOOCCH_2CH$), 42.38 (1C, $HOOCCH_2CHCO$), 52.71 (1C, $C_6H_5CHCH_2OCH_3$), 58.9 (CH_2OCH_3), 60.76 (1C, $CHC(CH_3)_3$), 74.9 (1C, CH_2OCH_3), 125.71-130.39 (13C, CH=CH), 135.11-141.93 (5C, CH=C=), 170.55-175.59 (2C, CONH, and 1C, COOH).

2.3. Synthesis of UK-370106-CO^{13}CHO

UK-370106-COOH was converted into UK 370106-$CO^{13}CHN_2$ using a procedure modified from that described by Cesar at al. [19]. N-[^{13}C]Methyl-N-nitrosotoluene-p-sulfonamide was used to generate ^{13}C-enriched diazomethane. Isobutylchloroformate (0.11 mmol) in anhydrous tetrahydrofuran (0.5 mL) was added, under a N_2 atmosphere, to the solution of the carboxylic acid (UK-370106-COOH) (0.1 mmol) and N-ethyldiisopropylamine (0.1 mmol) in tetrahydrofuran (5 mL) at -15 °C and the mixture was stirred for 30 minutes at -5°C. A solution of the ^{13}C-enriched diazomethane (100 mmol) in diethyl ether (30 mL) was added and the reaction mixture was stirred for 24 h at +4 °C. The formation of the diazoketone was monitored by thin layer chromatography (ethyl acetate/ petroleum ether /dichloromethane = 4/4/2). When the reaction was complete the solvent was evaporated under reduced pressure. The residue was dissolved in ethyl acetate and washed with 10% aqueous citric acid, saturated aqueous $NaHCO_3$ and saturated aqueous NaCl . The organic layer was dried over $MgSO_4$ and the solvent evaporated. The diazoketone was purified by silica gel chromatography using ethyl acetate / petroleum ether / dichloromethane = 4/5/1 as an eluent.

The diazoketone (UK-370106-$CO^{13}CHN_2$) was oxidised to the glyoxal using a procedure modified from that of Ihmels et al. [20]. 20 mg (0.034 mmol) of UK-370106-$CO^{13}CHN_2$ was oxidised by dissolving it in a 20 mL solution of 0.1 M dimethyldioxirane in acetone and stirring for ~ 2h at 0°C. The reaction mixture was then moistened, and the acetone removed by evaporation under reduced pressure. The moist compound was then dissolved in *d_6*-DMSO. In d_6-DMSO there were two ^{13}C-NMR signals, one small signal at 188.1 ppm and another larger signal at 90.8 ppm due to the ^{13}C-enriched glyoxal aldehyde carbon and its hydrate respectively. In water one signal at 90.4 ppm was observed due to the ^{13}C-enriched hydrated aldehyde carbon of the glyoxal group.

2.4. Isolation of the stromelysin-1 catalytic domain (residues 83-247).

The proMMP-3 catalytic domain complex was purified from *E. coli* (strain BL21(DE3)) that had been transformed with the pET-3A plasmid containing the gene for the proMMP-3 catalytic domain (residues 83-247). Cells were incubated at 37 ºC to an optical density of $A_{590} = 0.4 – 0.5$ and induced with 0.4 mM isopropyl β-thio-galactoside and then incubated at 37 ºC for 4 hours. The cells were

centrifuged and suspended in 500 mL of 50 mM Tris-HCl buffer at pH 8 containing, 100 mM NaCl and 0.27 g/litre lysozyme. It was then stirred overnight at room temperature. 0.625 g of deoxycholate was added and the solution was stirred for 1-2 hours. 0.5 mL of DNase 1 (1 mg/mL) was added and the solution was stirred for 1-2 hours. The solution was centrifuged and the pellet was washed three times with 50 mM Tris-HCl at pH 8 containing 100 mM NaCl and 0.5% (v/v) Triton-X100.

The pellet was dissolved in 20 mM Tris-HCl buffer at pH 8.6 containing 8 M urea, 20 mM 1, 4-dithiothreitol and 50 μM $ZnCl_2$ and then applied to a Macro-Prep High Q Support anion exchange column which had been equilibrated in 20 mM Tris-HCl buffer at pH 8.6 containing 8 M urea and 50 μM $ZnCl_2$. The column was washed with the same buffer, and the pro-stromelysin-1 was then eluted with the same buffer containing 1.5 M NaCl. The eluted protein was pooled and then dialyzed 3 x against 2 litres of 50 mM Tris-HCl at pH 7.5 containing 0.15 M NaCl, 10 mM $CaCl_2$, 50 μM $ZnCl_2$ and 0.02% (w/v) NaN_3. It was then dialyzed 2x against 2 litres of 50 mM Tris-HCL at pH 7.5 containing 10 mM $CaCl_2$, 50 μM $ZnCl_2$ and 0.02 % NaN_3 (w/v). Pro-stromelysin-1 was concentrated using an Amicon PBGC-10 membrane and activated by reacting with 1 mM 4-aminophenylmercuric acetate at 37 ºC for 16 hours [21]. ~50 mL of the activated stromelysin-1 was dialyzed against 2 litres of 50 mM MOPS buffer at pH 7.5 containing 10 mM $CaCl_2$ and 50 μM $ZnCl_2$. It was then dialyzed against 2x 1 litre 20 mM MOPS buffer at pH 7.5 containing 10 mM $CaCl_2$, and 50 μM $ZnCl_2$.

2.5. Catalytic activity and inhibition of SCD

The catalytic activity of SCD was determined by its ability to catalyze the hydrolysis of the thiopeptolide Acetyl-Proline-Leucine-Glycine- [2-mercapto-4-methyl-pentanoyl]-Leucine-Glycine-OC_2H_5 that was developed for assaying collagenase activity [22]. A 1000 μl assay contained 50 mM MOPS buffer at pH 6.0, 10 mM $CaCl_2$, 100 μM thiopeptolide substrate, 1 mM 5, 5'-dithiobis(2,2'-nitrobenzoic acid) and 3.3 % (v/v) dimethyl sulfoxide. The rate of cleavage of the thioester bond was determined by the reaction of 5,5'-dithiobis(2,2'-nitrobenzoic acid) with the thiol group formed on

hydrolysis of the thioester bond in the thiopeptolide substrate. The increase in absorbance at 412 nm due to the formation of 2-nitro-5-thiobenzoic acid was monitored on a Varian Cary 50 UV/Visible spectrophotometer at 25 ºC and the amount of 2-nitro-5-thiobenzoic acid was determined using ε_{412} = 13600 M^{-1} cm^{-1} [23].

The fluorescent substrate MCA-Arg-Pro-Lys-Pro-Val-Glu-Nva-Trp-Arg-Lys (Dnp)-NH_2 is one of the few fluorescent synthetic substrates specific for stromelysin-1 [24] and it was used to determine K_i values at different pHs. The SCD catalyzed hydrolysis of MCA-Arg-Pro-Lys-Pro-Val-Glu-Nva-Trp-Arg-Lys (Dnp)-NH_2 and its inhibition at a range of pH values was studied at 25 ºC using a 100 µl assay volume. The assays contained a 50 mM buffer (sodium acetate pH 5.0 -5.5, MES pH 6.0 - 6.50, MOPS pH.7.0 -7.5), 0.15 M NaCl, 10 mM $CaCl_2$ and 3.3 % (v/v) dimethyl sulfoxide. Stock solutions of substrates and inhibitors were dissolved in dimethyl sulfoxide. Fluorescence assays were carried out using a Spectramax M2 fluorescence spectrophotometer with excitation and emission wavelengths of 325 nm and 393 nm respectively at 25 ºC.

K_M values for the fluorescent substrate MCA-Arg-Pro-Lys-Pro-Val-Glu-Nva-Trp-Arg-Lys (Dnp)-NH_2 were estimated by initial rate measurements with substrate concentrations within the range 0.5-200µM. The initial rates obtained were fitted to the hyperbolic form of the Michaelis-Menten equation [25]. At pHs of 5.0, 6.0, 7.5 and 8.1 K_M values of 29.8 ± 3.4, 23.8 ± 2.9 µM, 45.8 ± 8.7 µM and 45.4 ± 5.2 µM respectively were estimated.

K_i values were estimated using a substrate concentration of 2 µM. Therefore $[S_0] << K_M$ and the equation for competitive inhibition $d[P]/dt=k_{cat}*[E]*[S]/([S]+ K_M*(1+[I]/ K_i))$ reduces to $d[P]/dt=(k_{cat}/K_M) *[E]*[S]* K_i/([I]+ K_i)$. K_i values were estimated by using a nonlinear least squares regression program [26].

2.6. Concentrations of SCD

Enzyme concentrations were determined using the ε_{280} value of 28700 $M^{-1}cm^{-1}$ determined in the Results section.

2.7. NMR Spectroscopy

NMR spectra at 11.75 T were recorded with a Bruker Avance DRX 500 standard-bore spectrometer operating at 125.7716 MHz for ^{13}C-nuclei. 5 mm-diameter Shigemi NMR tubes containing 0.32-0.34 mL samples were used for ^{13}C-NMR spectroscopy. The ^{13}C-NMR spectral conditions for the samples of the UK-370106-CO^{13}CHO inhibitor with or without SCD were: 8192 time domain data points; spectral width 236.6 ppm; acquisition time 0.138 s; 0.65 s relaxation delay time; 90º pulse angle; 4096 transients recorded per spectrum. Waltz- 16 composite pulse ^{1}H decoupling of 0.4 watts was used which was reduced to 0.006 watts during the relaxation delay to minimize dielectric heating but maintain the Nuclear Overhauser Effect. Unless stated otherwise all spectra were transformed using an exponential weight factor of 20 Hz.

^{1}H-NMR spectra were obtained at 500 MHz using 5 mm-diameter Shigemi NMR tubes and containing 0.32-0.34 mL samples. The ^{1}H-NMR spectral conditions for the samples of free SCD and SCD inhibited by UK-370106-COOH or UK-370106CO^{13}CHO at 11.75 T were: 32768 time-domain data points; spectral width 40 ppm; acquisition time 0.82 s; 1.0 s relaxation delay time; 90° pulse angle; 256 transients were recorded per spectrum. Water suppression was achieved using the Watergate W5 pulse sequence with gradients [27]. Spectra were transformed using an exponential weighting factor of 50 Hz. ^{13}C-NMR spectra confirming the formation of the SCD inhibitor complex with the UK-370106-CO^{13}CHO glyoxal inhibitor were obtained prior to ^{1}H-NMR studies.

Both ^{1}H and ^{13}C chemical shifts are quoted relative to tetramethylsilane at 0.00 ppm. The chemical shift of d_6-dimethyl sulfoxide at 38.7 ppm was used as a secondary reference in aqueous solutions. Aqueous samples contained 10% (v/v) $^{2}H_2O$ to obtain a deuterium lock signal. Due to the susceptibility of SCD to acid or alkaline denaturation we could not adjust sample pHs using NaOH or HCl. Therefore all pH adjustments of NMR samples containing stromelysin-1 were made using small amounts of 1M acetate, MOPS, MES or HEPES buffers.

3. Results

3.1 Properties of the Stromelysin-1 catalytic domain 83-247

The protein concentration of the unfolded stromelysin-1 catalytic domain 83-247 in 6 M guanidine hydrochloride containing 0.02 M phosphate buffer at pH 6.5 was estimated using an ε_{280} value of 27310 $M^{-1}cm^{-1}$ calculated from the expected extinctions of the 3 tryptophan and 8 tyrosine residues [28] of the stromelysin-1 catalytic domain 83-247. This extinction was use to determine the concentration of a sample of the active SCD when it was dissolved in 6 M guanidine hydrochloride containing 0.02M phosphate buffer at pH 6.5. By measuring absorbance of the same amount of the active stromelysin-1 catalytic domain 83-247 in water at pH 7.5 we estimate that in water at pH 7.5 the native stromelysin-1 catalytic domain 83-247 has an ε_{280} value of 28700 ± 900 $M^{-1}cm^{-1}$ (Mean of 6 determinations). This is in good agreement with the values of 28790 and 28460 $M^{-1}cm^{-1}$ determined previously [29, 30] for the stromelysin-1 catalytic domain containing the residues 83-256. As both these catalytic domains contain the same number of tryptophan, tyrosine and cysteine residues they are expected to have the same extinction coefficients at 280 nM [28].

Using MALDI-TOF mass spectrometry the stromelysin-1 catalytic domain 83-247 had a M_r value of 18572.5, which is in good agreement with the value of 18574.8 expected on the basis of its amino acid sequence. On SDS-Page the stromelysin-1 catalytic domain 83-247 migrated as if it had a larger M_r value of 21,500. A similar result was obtained with the stromelysin-1 catalytic domain 83-255 (M_r 19395.6) which migrated on SDS-Page as if it had an even larger M_r value of 23,500[31].

When SCD was assayed using the thiopeptolide substrate Ac-Pro-leu-Gly-thioester-Leu-Leu-Gly-OC_2H_5 at 25°C and pH 6.0 the estimated catalytic parameters k_{cat} and K_M were 2.60 ± 0.13 s^{-1} and 395 ± 54 μM respectively. These values are in reasonable agreement with earlier values obtained for k_{cat} and K_M respectively for full length stromelysin-1 and for the stromelysin-1 catalytic domain 83-256 (Table 1). The stoichiometry of the ^{13}C-NMR titration of SCD with UK-370106-CO^{13}CHO confirmed that our SCD preparations were fully active.

3.2. ^{13}C-NMR of the UK-370106-CO^{13}CHO inhibitor in d_6-dimethyl sulfoxide and aqueous solutions

In d_6-dimethyl sulfoxide the UK-370106-$CO^{13}CHO$ inhibitor (Scheme 1) gave two signals: one large signal at 90.8 ppm (J_{CH} 161.3 ± 0.1 Hz) due to the sp^3 hybridized hemiacetal carbon of the hydrated glyoxal aldehyde carbon (Structures (a) or (b) in Scheme 2) and a smaller signal at 188.1 ppm. (J_{CH} 187.7 ± 0.1 Hz) due to the sp^2 hybridized aldehyde carbon of the non-hydrated glyoxal (Structure (c) in Scheme 2). The hydration constant of the glyoxal keto group in peptide glyoxals is 70 x less than that of the glyoxal aldehyde group [11]. Therefore we expect that species (b) and (c) in Scheme 2 will be the major species in d_6-dimethyl sulfoxide. In aqueous solutions containing 20-30% d_6-dimethyl sulfoxide a single signal at 90.4 ppm (J_{CH} 163.0 ± 0.1 Hz) was observed (Fig. 3b) showing that the glyoxal aldehyde carbon was fully hydrated in aqueous solutions (Structures (a) and (b) in Scheme 2). In aqueous solutions the aldehyde carbon of a peptide glyoxal is usually approximately 100% hydrated (K_{HYD}=[HYDRATE]/[NONHYDRATE] = 89.3) and the keto carbon is approximately 50% hydrated (K_{HYD} = 1.3) [11]. Therefore the hydrated aldehyde carbon of the glyoxal gives signals at ~90.2 ppm and ~88.7 ppm when the glyoxal keto carbon is hydrated (Structure (d) in Scheme 2) and non-hydrated (Structure (e) in Scheme 2) respectively[1-4, 6, 9, 12]. As only one signal is observed when the UK-370106-$CO^{13}CHO$ inhibitor is dissolved in aqueous media we can conclude that either $K_{HYD} >> 1$ or $K_{HYD} << 1$ and either the glyoxal keto carbon predominates (Structure (b) in Scheme 2) or the hydrated keto carbon (Structure (a) in Scheme 2) predominates. The chemical shift value of 90.4 ppm for the UK-370106-$CO^{13}CHO$ inhibitor is similar to that observed (~90.2 ppm) for the hydrated aldehyde carbon of fully hydrated peptide glyoxals (Structure (d) in Scheme 2) suggesting that the fully hydrated form of the UK-370106-$CO^{13}CHO$ inhibitor (Structure (a) in Scheme 2) predominates in aqueous solutions.

Stability of the stromelysin-1 catalytic domain at pH 7.5.

In 10 mM MOPS buffer at pH 7.5 containing 10 mM CaCl2 the enzyme lost 40% of its catalytic activity after freezing and thawing, repeating the process results in the original catalytic activity being reduced by 70%. Therefore we did not freeze stromelysin-1 solutions. At 4 ˚C stromelysin-1 retained 95% of its catalytic activity after 102 days. Therefore the enzymes was stored at 4 ˚C before being used.

3.3. Effect of pH on the stability of SCD at 25 °C

At pHs 7.0 (Fig. 1A) and 8.0 (Fig. 1B) there was no decrease in catalytic activity with time. There was an initial 6-9% decrease in activity at pHs 6.0 (Fig. 1A) and 8.4 (Fig. 1B) but then the catalytic activity was stable. At pH 5.5 there was an initial 6% decrease in catalytic activity followed by a linear decrease in catalytic activity (Fig. 1A). There was an exponential decrease in catalytic activity at pH values of 5 (Fig.3A) and 9 (Fig. 1B). At pHs 4.5 (Fig. 1A) and 10.0 (Fig. 1B) the decrease in activity was biphasic there was rapid exponential loss of the first 60-66% of catalytic activity but after that the exponential decrease in catalytic activity was 10-40 times slower.

At pHs 6-8 SCD samples lost less than 10 % of their catalytic activity in 960 min (Fig. 1 A,B). In order to observe the ^{13}C-NMR signal from the ^{13}C-enriched carbon of UK-370106-CO^{13}CHO bound to SCD, NMR spectra were accumulated over a 54 minute period. After 1 hour at pH 5.5 SCD samples retained 90% of their catalytic activity but at pH 5.0 only 36% of their catalytic activity was retained after 1 hour (Fig. 1A). Therefore our NMR studies were restricted to pH values of 5.5 or higher (Fig.s 4 & 5). After 1 hour at pH 8.4 SCD samples retained 89% of their catalytic activity but at pH 9.0 only 52 % of their catalytic activity remained after one hour (Fig. 1B). Therefore our NMR studies were restricted to pH values of 8.4 or less (Fig.s 4 & 5). For initial rate measurements at pHs 5-9 there was no detactable loss of catalytic activity over a 5 minute period. However at pH 4.5 initial rates were measured over a 2 minute period during which there was no more than a 10% loss of catalytic activity. The rapid rate of acid denaturation at pH 4 and below prevented studies at pH 4 or lower.

3.4. Effect of pH on the binding of UK-370106-CO^{13}CHO to SCD

K_i values were minimal at pHs 5.5-6.5 but increased at lower or higher pHs (Fig. 2A). A plot of $1/K_i$ versus pH (Fig. 2B) was bell shaped and the fitted pK_a values were 5.9 ± 0.4 and 6.2 ± 0.4 for pK_1 and pK_2 respectively. These free enzyme pK_a values are very similar to the values of 5.4-5.8 and 6.0-6.3 obtained from plots of $1/K_i$ versus pH with other inhibitors [32]. Plots of k_{cat}/K_M versus pH give similar free enzyme pK_a values for pK_1 and pK_2 and they also give an additional pK_a of 8.5-9.9 [32,

33]. From the pH dependence of the K_i values (Fig. 2A) it was estimated the increases in K_i at acid and alkaline pHs depended on pK_a values of 4.4 ± 1.5 and 7.5 ± 0.2 respectively. Due to the large error associated with the value of pK_1 (4.4 ± 1.5) obtained from the pH dependence of K_i we do not know if pK_1 is significantly perturbed by inhibitor binding. The pK_a of 7.5 suggests that inhibitor binding increases pK_2 by 1.3 pK_a units.

3.5. ^{13}C-NMR of SCD inhibited by UK-370106-CO^{13}CHO

On adding UK-370106-CO^{13}CHO (Fig. 3b) to SCD (Fig. 3a) at pH 7.0 a new signal at 92.0 ppm was detected (Fig. 3c). Carbons with directly bonded protons relax predominantly by dipolar relaxation and linewidths are directly proportional to M_r values provided the carbon is rigidly bound [34, 35]. When the fully hydrated inhibitor (Structure (a) in Scheme 2, M_r 620) binds to the SCD (83-247, M_r 18575) we expect an increase in linewidth of 20-35 Hz [34, 36]. The observed increase in linewidth was 20 ± 7 Hz confirming that the UK-370106-CO^{13}CHO inhibitor is tightly bound to SCD. The chemical shift value of 92.0 ppm confirms that the inhibitor glyoxal aldehyde carbon is sp^3 hybridised and therefore the glyoxal aldehyde group must be fully hydrated when it is bound to SCD. The UK-370106-COOH is a potent inhibitor of SCD (Table 2) and so it should displace the less tightly bound glyoxal inhibitor UK-370106-COCHO inhibitor (Table 2). Adding approximately equimolar UK-370106-COOH led to loss of the signal at 92.0 ppm due to the bound glyoxal inhibitor and re-appearance of the signal at 90.4 ppm due to the free glyoxal inhibitor (Fig. 3d). This confirms that the glyoxal inhibitor is reversibly bound at the active site of SCD.

3.6. Effect of pH on the ^{13}C-NMR signal from the ^{13}C-enriched carbon of UK-370106-CO^{13}CHO inhibitor bound to SCD

The chemical shift of the signal due to the ^{13}C-enriched carbon of the bound inhibitor did not change significantly from pH 5.52 to 8.44 (only changed 0.1 ppm, Fig. 4). However, the intensity of this signal changed significantly with pH (Fig. 4) and showed a bell shaped pH dependence (Fig. 5) with signal intensity increasing according to a pK_a of 5.8± 0.2 to a maximum value at pH 6.75 then decreasing in intensity according to a pK_a of 7.8 ± 0.2 at alkaline pHs .

Based on the experimentally determined K_i value of 0.81 μM at pH 5.53 we estimate that 99.4% of SCD will be saturated with the glyoxal inhibitor at this pH. This, plus the fact that no free inhibitor signals at 90 .4 ppm were detected at low pH, confirms that the decrease in signal intensity at low pH (Fig.s 4 & 5) cannot be attributed to the disassociation of the SCD-UK-370106-CO^{13}CHO inhibitor complex. The pK_a of 7.8 ± 0.2 for the decrease in signal intensity at alkaline pH values is very similar to the pK_a of 7.6 ± 0.2 for the increase in K_i values at alkaline pHs (Fig. 2a). This suggests that the decrease in the intensity of the signal from the UK-370106-CO^{13}CHO inhibitor bound to SCD is due to the disassociation of the inhibitor complex at alkaline pHs. This was confirmed by the fact that the release of free inhibitor at 90.41 ppm was observed at alkaline pHs (Fig. 4e, f). Both bound and free inhibitor were observed in our ^{13}C-NMR experiments at pHs 7.54 (Fig. 4e) and 7.96 (Fig. 4f). These signals were lost at higher pHs (Fig. 4g) due to breakdown of the free glyoxal inhibitor at high pH [1]. The fact that we can observe clearly resolved signals from both the free (90.4 ppm) and bound (~92.0 ppm) inhibitor when the K_i is approx. 20 μM shows that the rate of association of SCD and the UK-370106-CO^{13}CHO inhibitor must be no greater than 2 x 10^6 $M^{-1}. s^{-1}$ at pHs 7.5-8.0. If the rate of association were 2 x 10^7 $M^{-1}. s^{-1}$ the signals due to the free and bound inhibitor would coalesce and a single signal would be observed.

3.7. ^{1}H-NMR of the hydrogen-bonded protons of SCD, a SCD-UK-370106-COOH complex, and a SCD-UK-370106-CO^{13}CHO complex

Hydrogen bonded protons have chemical shifts in the range 11-22 ppm and with SCD 7 signals were observed with chemical shifts > 11 ppm (Fig. 6A). These signals had chemical shifts of 11.4, 11.6, 11.8, 12.3, 12.9, 13.1 and 13.5 ppm (Fig. 6A). As the pH increased the intensity of the signals at 12.9, 13.1 and 13.5 decreased (Fig.s 6A, spectra 1-6) but these intensities were restored when the pH was lowered to pH 6.7 (spectrum not shown). As the positions of the signals did not change with pH, this decrease in intensity must be controlled by a slow exchange process. The pK_a values of 7.94, 6.67 and 7.49 controlling the decrease in intensity of the signals at 12.9, 13.1 and 13.5 ppm respectively (Table 3), are significantly larger than pK_1 (5.4-5.8) and pK_2 (6.0-6.3) and smaller than pK_3 (8.5-9.9) determined from the pH dependence of k_{cat}/K_M [32, 33]. It is therefore unlikely that

these hydrogen bonded protons play a direct role in catalysis. On binding the UK-370106-COOH (Fig. 6B) or UK-370106-CO^{13}CHO (Fig. 6C) inhibitors the signal at 12.9 ppm was no longer resolved. However the intensity of the signal at 13.1 increased suggesting these signals may have merged.

On adding UK-370106-COOH a new signal at 12.1 ppm was resolved (Fig. 6B, spectrum 4). This signal was not observed when the UK-370106-CO^{13}CHO inhibitor was added to SCD and so it would appear to represent a unique hydrogen bond formed between SCD and the UK-370106-COOH inhibitor. However, we cannot dismiss the possibility that this signal is present in the free enzyme and glyoxal complex but it is merged with other signals and only when the UK-370106-COOH inhibitor binds is the signal at 12.1 ppm resolved. The signal at 11.6 in SCD (Fig. 6A, spectrum 2) and in the SCD-UK-370106-COOH inhibitor complex (Fig. 6B, spectrum 2) was not resolved when the UK-370106-CO^{13}CHO inhibitor was added to SCD (Fig. 6C) which may simply reflect the fact that it may have merged with signal at 11.4 ppm. The binding of inhibitors to SCD increased the pK_a values controlling the intensity of the signal at 13.1 ppm (Table 3). If the binding of the inhibitors increases the hydrophobicity of the environment of the ionizing group then this increase in pK_a would suggest that the ionizing group controlling the intensity of the signal at 13.1 ppm is a neutral acid such as a carboxylate group. As inhibitor binding causes the pK_a controlling the intensity of the signal at 13.5 ppm to stay the same or decrease then this suggests that the ionizing group controlling the intensity of the signal at 13.5 ppm is a cationic acid such as the imidazolium group of a histidine residue.

Strongly hydrogen bonded protons have chemical shifts of 16-20 ppm and are called low-barrier hydrogen bonds [37]. It is clear from our results that there are no low barrier hydrogen bonds in SCD (Fig. 6A) and none are formed when SCD binds the UK-370106-COOH (Fig. 6B) or UK-370106-CO^{13}CHO (Fig. 6C) inhibitors.

Discussion

For most metalloproteinases the pH dependence of k_{cat}/K_M is bell shaped being dependant on three protonic states (EH_2, EH and E) with the EH state being the catalytically active form (Scheme 3A) whose formation is governed by pK_1 and whose breakdown is governed by pK_2 [38]. However, for SCD the pH dependance of k_{cat}/K_M is more complex [32, 33, 38] being dependent on 4 protonic states (EH_3, EH_2, EH and E) with two catalytically active states (EH_2 and EH) whose formation and breakdown are controlled by the free enzyme pK_as pK_1, pK_2 and pK_3 (Scheme 3B). pK_1, pK_2 and pK_3 give free enzyme pK_a values of 5.2-5.8, 6.0-6.3 and 8.7-9.9 respectively [32, 33, 38]. pK_1 has been assigned to a Glu-202-zinc-water complex [32, 33, 38] and pK_3 is assigned to Tyr-223 [38]. Using site directed mutagenesis pK_2 has been shown to be due to His-224 which is thought to stabilize the enzyme structure by hydrogen bonding to a main chain peptide carbonyl group [32, 38]. Replacement of His-224 with a glutamine residue increases catalytic activity and gives a bell shaped pH profile for k_{cat}/K_M showing that ionisation of His-224 decreases catalytic activity[38]. Therefore only pK_1 is thought to be directly involved in catalysis while pK_2 controls deprotonation of His-224 by reducing but not eliminating catalytic activity, pK_3 controls deprotonation of Tyr-223 which eliminates catalytic activity. In both cases (pK_2 and pK_3) deprotonation is thought to cause conformational changes that reduce catalytic activity.

The binding of inhibitors is dependent on both pK_1 and pK_2 [32]. These studies [32] used 5,5'-dithiobis-(2-nitrobenzoic acid) to quantify the rate of thiopeptolide substrate hydrolysis which limited them to pHs 5-8 due to the susceptability of 5, 5'-dithiobis-(2-nitrobenzoic acid) to alkaline hydrolysis and to the decrease in extinction of the 2-nitro-5-thiobenzoic acid at low pH (pK_a 4.5). Our studies with the fluorescent substrate MCA-Arg-Pro-Lys-Pro-Val-Glu-Nva-Trp-Arg-Lys(Dnp)-NH_2 were not subject to these limitations and were only limited by the pH stability of SCD and so could be extended to pH 4.5-9 for catalytic measurements. In free SCD pK_1 reflects ionization of the bound water in the Glu-202-zinc-water complex. However, when the UK-370106-CO^{13}CHO inhibitor is bound we expected that the zinc bound water would be replaced by the inhibitor glyoxal

group. The hydroxyl groups of the glyoxal hemiacetal and hemiketal groups are less basic than water by 3.5-6 pK_a units [1, 3] and so would be expected to have pK_a values 3.5-6.0 pK_a units lower than 5.9 (pK_1) when bound to zinc and so we would expect the glyoxal hemiacetal hydroxyl groups to be fully ionised at pHs 5.5-8.5 if they are coordinated to the active site zinc. However, at pH 5.5-8.5 the hemiacetal carbon of the inhibitor glyoxal group has a chemical shift of 91.89-91.99 ppm (Fig. 4). When glyoxal inhibitors are bound to chymotrypsin ionisation of the glyoxal hemiacetal hydroxyl groups in the presence of the positively charged active site histidine residue produces a titration shift from ~91 to ~97 ppm [1, 4]. Similar titration shifts are therefore expected if the positively charged active site zinc is coordinated to the glyoxal hemiacetal hydroxyl groups. The observed chemical shifts of ~92 ppm (Fig. 4) show that the inhibitor glyoxal hemiacetal hydroxyl groups are not ionised when bound to SCD at pHs 5.52-8.44. Therefore we conclude that we have found no evidence that glyoxal hemiacetal hydroxyl groups are directly coordinated to the active site zinc atom.

If the glyoxal hemiketal hydroxyl groups are coordinated to the active site zinc of stromelysin-1 then the increase in intensity of the signal at 92 ppm with a pKa ~5.8 (Fig. 5) could reflect the binding/ionisation of the glyoxal hemiketal hydroxyl groups when the glyoxal inhibitor binds to stromelysin-1. Ionisation of the hydroxyl groups of the glyoxal hemiketal group are expected to produce titration shifts of ~1.88 ppm (2 x 0.94 ppm, [3]) at the glyoxal hemiacetal carbon. If we assume fast exchange and a titration shift of 90.12 to 92 ppm controlled by a pK_a of 5.8 then a titration shift of 1.25 ppm would be observed from pH 5.5 to 8.5. The observed titration shift of 0.1 ppm (91.89-91.99) from pH 5.55 to 8.44 (Fig. 4) is negligible and so we cannot assign the pK_a of 5.8 (Fig. 5) to ionisation of the glyoxal hemiketal hydroxyl groups by fast exchange. If ionisation of the glyoxal hemiketal hydroxyl groups was a slow exchange process then we should have observed a signal at ~90.1 at low pH whose intensity would decrease according to a pK_a of 5.8 as there was a concommittant increase in the intensity of the signal at 92 ppm also according to a pK_a of 5.8. No additional signal at ~90.1 ppm was observed at low pH (Fig. 4) confirming that the pK_a of 5.8 does not reflect the ionisation of the glyoxal hemiketal hydroxyl groups. The pK_a values of glyoxal hemiketal hydroxyl groups are about 5-6 pK_a units lower than the pK_a of the hydroxyl

group of water [1, 3]. Therefore if the hemiketal hydroxyl groups interact with active site zinc atom in the same way as the hydroxyl group of water then we would expect that the glyoxal hemiketal hydroxyl groups would have a pK_a value of 2.4 or less and so it is possible that the glyoxal hemiketal hydroxyl groups are ionised and coordinated to the active site zinc atom. However, if the glyoxal group was coordinated to the zinc atom we would expect the glyoxal hemiacetal hydroxyl groups to also be ionised with the hemiacetal carbon having a chemical shift of ~97 ppm which is not observed. We have also shown that when a glyoxal inhibitor binds to pepsin there is an increase in chemical shift of the glyoxal hemiacetal carbon from 89.8 to 90.9 even though both the hemiacetal and hemiketal hydroxyl groups are not ionised in the free and bound glyoxal [9]. The increase in chemical shift of the glyoxal hemiacetal carbon from 90.4 to 92.0 ppm on binding the UK-370106-CO^{13}CHO inhibitor to SCD is similar in magnitude and can be attributed to the difference in the environment of the free and bound species.

Therefore all our experimental evidence suggests that the inhibitor glyoxal group is not directly coordinated to the catalytic zinc atom. The fact that the glyoxal inhibitor is a 500-fold weaker inhibitor than its parent carboxylate inhibitor supports this interpretation.Therefore we propose that the glyoxal inhibitor has not displaced the active site water molecule. In this case the pK_a of 5.8 reflects ionisation of this water molecule and binding of the glyoxal inhibitor has not significantly perturbed pK_1 from its expected value of 5.4-5.8 in free SCD [32].

pK_2 is assigned to His-224 which in its protonated form is thought to stabilise the S_1' subsite of SCD by hydrogen bonding to a peptide carbonyl group [32, 38]. As histidine is a cationic acid its pK_a is not expected to be affected by the changes in the hydrophobicity of its environment due to inhibitor binding. However on binding the UK-370106-CO^{13}CHO inhibitor, pK_2 is raised from 6.2 to 7.5. This suggests that this pK_a is not due to a cationic group such as the imidazolium group of His-224. However, increases in histidine pK_a values on ligand binding are observed in the serine proteases [4] when the imidazolium ion forms an ion pair with a carboxylate group. Therefore the increase in pK_2 suggests that on binding the UK-370106-CO^{13}CHO inhibitor the interaction of histidine-224 with a negatively charged group is enhanced. The alternative possibility that the pK_a of

7.5 is due to pK_3 being lowered also requires that pK_2 be suppressed which we consider unlikely. pK_3 is due to the hydroxyl group of the tyrosine-223 residue and as it is a neutral acid its pK_a is expected to increase if binding of a ligand increases the hydrophobicity of its environment. It is therefore unlikely that pK_3 has decreased to 7.5 on inhibitor binding as this would be expected to increase the hydrophobicity of its environment and so increase its pK_a. Therefore we assign the pK_a of 7.5 to pK_2.

The association rate constant for glyoxal inhibitors binding to the serine proteases has been shown to be at least 100 x slower than the diffusion controlled rate constant of 10^8 $M^{-1}s^{-1}$ [2, 4, 12]. These slow association rate constants are expected because inhibition of the serine proteases by glyoxal inhibitors involves the reversible formation of a hemiketal adduct between the active site serine hydroxyl group and the keto-carbon of the inhibitor glyoxal group [1]. However, it is surprising that with the aspartyl protease pepsin [9] and with the metalloprotease SCD the association rate constant of glyoxal inhibitors is also at least a 50 x slower than the diffusion controlled rate constant. Hydration and dehydration of carbonyl groups is a slow process [39]. The peptide glyoxal inhibitor is bound to the the aspartyl protease pepsin in its fully hydrated form and so the slow association rate in this case may be due to the slow rate of hydration of the glyoxal keto-carbon. Likewise with SCD the slow association rate could reflect the slow rate of hydration or dehydration of the glyoxal inhibitor. Our NMR results with SCD and the UK-370106-CO^{13}CHO inhibitor show that the glyoxal aldehyde carbon is fully hydrated in both the free and the bound inhibitor. Therefore if association involves a slow hydration-dehydration step then this must be at the glyoxal keto-carbon. If, as we argued, the free UK-370106-CO^{13}CHO inhibitor is fully hydrated in water then this suggests that the keto-carbon of the glyoxal inhibitor might be dehydrated when it is bound to SCD. It is also possible that the slow association rate could be because inhibitor binding involves a slow conformational change as has been observed with inhibitors binding to other metalloproteinases such as the gelatinases [40].

Prostromelysin-1 is a 57 kDa protein which is activated by removal of 82 amino acid residues from the N-terminus by proteolysis. This produces catalyically active 45 kDa stromelysin-1

containig residues 83-477 [21]. It has been reported [33] that at 25 °C stromelysin-1 (residues 83-477) retains full catalytic activity for 15 hours at pHs 5.5 to 9.5. For stromelysin-1 C-terminal truncated stromelysin-1(residues 83-255) at 37 °C it has been shown that after an initial ~20% decrease in catalytic activity the enzyme is stable at pHs 6-9 for at least 6 hours [41]. The C-terminal truncated stromelysin-1 (residues 83 to 247) used in this work was stable at 25 °C for at least 16 hours from pH 6 to pH 8.4 (Figs.1A,B). Therefore we conclude that at 25 °C , C-terminal truncation decreases the stability of the stromelysin-1 catalytic domain at pH values > 8.4 and < 6.0. However, the active truncated enzyme has essentially the same catalytic properties as the non-truncated enzyme.

Acknowledgements

This work was supported by a Research Frontiers Programme grant 05/RF/BIC026 from Science Foundation Ireland and by a grant from the Programme for Research in Third-Level Institutions (PRTLI-4). Funding from Science Foundation Ireland was used to purchase and upgrade the 500 MHz NMR spectrometer used in these studies. We thank University College Dublin for a President's Research Fellowship for Prof. J. Paul. G. Malthouse.

We would like to acknowledge the expert advice of Dr Robert Visse in expressing and isolating SCD. We would also like to thank Professor Hideaki Nagase for the generous gift of a pET3a plasmid containing the recombinant SCD catalytic domain containing residues 83-247.

References

[1] A. Djurdjevic-Pahl, C. Hewage, J.P.G. Malthouse, A ^{13}C-NMR study of the inhibition of delta-chymotrypsin by a tripeptide-glyoxal inhibitor, Biochem. J. 362 (2002) 339-347.

[2] A. Djurdjevic-Pahl, C. Hewage, J.P.G. Malthouse, Ionisations within a subtilisin-glyoxal inhibitor complex, Biochim. Biophys. Acta 1749 (2005) 33-41.

[3] N. Howe, L. Rogers, C. Hewage, J.P.G. Malthouse, Oxyanion and Tetrahedral Intermediate Stabilization by subtilisin: detection of a new tetrahedral adduct, Biochimica et Biophysica Acta (BBA) - Proteins & Proteomics 1794 (2009) 1251-1258.

[4] E. Spink, S. Cosgrove, L. Rogers, C. Hewage, J.P. Malthouse, ^{13}C and ^{1}H NMR studies of ionizations and hydrogen bonding in chymotrypsin-glyoxal inhibitor complexes, J. Biol. Chem. 282 (2007) 7852-7861.

[5] B. Walker, N. McCarthy, A. Healy, T. Ye, M.A. McKervey, Peptide glyoxals: a novel class of inhibitor for serine and cysteine proteinases, Biochem. J. 293 (1993) 321-323.

[6] J. Lowther, A. Djurdjevic-Pahl, C. Hewage, J.P.G. Malthouse, A ^{13}C-NMR study of the inhibition of papain by a dipeptide-glyoxal inhibitor, Biochem. J. 366 (2002) 983-987.

[7] J.F. Lynas, S.J. Hawthorne, B. Walker, Development of Peptidyl a-keto-b-aldehydes as New Inhibitors of Cathepsin L-Comparisons of Potency and Selectivity Profiles with Cathepsin B, Bioorg. Med. Chem. Lett. 10 (2000) 1771-1773.

[8] B. Walker, J.F. Lynas, M.A. Meighan, D. Bromme, Evaluation of Dipeptide a-Keto-b-aldehydes as New Inhibitors of Cathepsin S, Biochem. Biophys. Res. Commun. 275 (2000) 401-405.

[9] S. Cosgrove, L. Rogers, C. Hewage, J.P. Malthouse, An NMR study of the inhibition of pepsin by glyoxal inhibitors: Mechanism of tetrahedral intermediate stabilization by the aspartyl proteinases, Biochemistry 46 (2007) 11205-11215.

[10] D. Qasmi, E. de Rosny, L. Rene, B. Badet, I. Vergely, N. Boggetto, M. Reboud-Ravaux, Synthesis of N-glyoxylyl peptides and their in vitro evaluation as HIV-1 protease inhibitors, Bioorganic & Medicinal Chemistry 5 (1997) 707-714.

[11] E. Spink, C. Hewage, J.P. Malthouse, Determination of the structure of tetrahedral transition state analogues bound at the active site of chymotrypsin using ^{18}O and ^{2}H isotope shifts in the ^{13}C NMR spectra of glyoxal inhibitors, Biochemistry 46 (2007) 12868-12874.

[12] J.P. Malthouse, ^{13}C- and ^{1}H-NMR studies of oxyanion and tetrahedral intermediate stabilization by the serine proteinases: optimizing inhibitor warhead specificity and potency by studying the inhibition of the serine proteinases by peptide-derived chloromethane and glyoxal inhibitors, Biochem. Soc. Trans. 35 (2007) 566-570.

[13] B. Lovejoy, A.M. Hassell, M.A. Luther, D. Weigl, S.R. Jordan, Crystal structures of recombinant 19-kDa human fibroblast collagenase complexed to itself, Biochemistry 33 (1994) 8207-8217.

[14] B.W. Matthews, Structural Basis of the Action of Thermolysin and related Zinc Peptidases, Acc. Chem. Res. 21 (1988) 333-340.

[15] W.L. Mock, D.J. Stanford, Arazoformyl dipeptide substrates for thermolysin. Confirmation of a reverse protonation catalytic mechanism, Biochemistry 35 (1996) 7369-7377.

[16] M. Whittaker, C.D. Floyd, P. Brown, A.J. Gearing, Design and therapeutic application of matrix metalloproteinase inhibitors, Chem. Rev. 99 (1999) 2735-2776.

[17] C.P. Ashcroft, S. Challenger, A.M. Derrick, R. Storey, N.M. Thomson, Asymmetric Synthesis of an MMP-3 Inhibitor Incorporating a 2-Alkyl Succinate Motif, Organic Process Research & Development 7 (2003) 362-368.

[18] M.J. Fray, R.P. Dickinson, J.P. Huggins, N.L. Occleston, A potent, selective inhibitor of matrix metalloproteinase-3 for the topical treatment of chronic dermal ulcers, J. Med. Chem. 46 (2003) 3514-3525.

[19] J. Cesar, M.S. Dolene, Trimethylsilyldiazomethane in the preparation of diazoketones via mixed anhydride and coupling reagent methods: a new approach to the Arndt-Eistert synthesis, Tetrahedron Lett. 42 (2001) 7099-7102.

[20] H. Ihmels, M. Maggini, M. Prato, G. Scorrano, Oxidation of Diazo Compounds by Dimethyl Dioxirane:an Extremely Mild and Efficient Method for the Preparation of Labile a-Oxo-Aldehydes, Tetrahedron Lett. 32 (1991) 6215-6218.
[21] H. Nagase, J.J. Enghild, K. Suzuki, G. Salvesen, Stepwise activation mechanisms of the precursor of matrix metalloproteinase 3 (stromelysin) by proteinases and (4-aminophenyl)mercuric acetate, Biochemistry 29 (1990) 5783-5789.
[22] H. Weingarten, J. Feder, Spectrophotometric assay for vertebrate collagenase, Anal. Biochem. 147 (1985) 437-440.
[23] G.L. Ellman, Tissue sulfhydryl groups. , Arch. Biochem. Biophys. 82 (1959) 70-77.
[24] H. Nagase, C.G. Fields, G.B. Fields, Design and characterization of a fluorogenic substrate selectively hydrolyzed by stromelysin 1 (matrix metalloproteinase-3), J. Biol. Chem. 269 (1994) 20952-20957.
[25] G.N. Wilkinson, Statistical estimations in enzyme kinetics, Biochem J 80 (1961) 324-332.
[26] J.P.G. Malthouse, W.U. Primrose, N.E. Mackenzie, A.I. Scott, ^{13}C NMR Study of the Ionizations within a Trypsin-Chloromethyl Ketone Inhibitor Complex, Biochemistry 24 (1985) 3478-3487.
[27] M. Liu, X. Mao, C. He, H. Huang, J.K. Nicholson, J.C. Lindon, Improved WATERGATE Pulse Sequences for Solvent Suppression in NMR Spectroscopy, J. Magn. Reson. 132 (1998) 125-129.
[28] S.C. Gill, P.H. von Hippel, Calculation of protein extinction coefficients from amino acid sequence data, Anal. Biochem. 182 (1989) 319-326.
[29] M.H. Parker, E.A. Lunney, D.F. Ortwine, A.G. Pavlovsky, C. Humblet, C.G. Brouillette, Analysis of the binding of hydroxamic acid and carboxylic acid inhibitors to the stromelysin-1 (matrix metalloproteinase-3) catalytic domain by isothermal titration calorimetry, Biochemistry 38 (1999) 13592-13601.
[30] S.P. Salowe, A.I. Marcy, G.C. Cuca, C.K. Smith, I.E. Kopka, W.K. Hagmann, J.D. Hermes, Characterization of zinc-binding sites in human stromelysin-1: stoichiometry of the catalytic domain and identification of a cysteine ligand in the proenzyme, Biochemistry 31 (1992) 4535-4540.
[31] K. Suzuki, C.C. Kan, W. Hung, M.R. Gehring, K. Brew, H. Nagase, Expression of human pro-matrix metalloproteinase 3 that lacks the N-terminal 34 residues in Escherichia coli: autoactivation and interaction with tissue inhibitor of metalloproteinase 1 (TIMP-1), Biol. Chem. 379 (1998) 185-191.
[32] L.L. Johnson, A.G. Pavlovsky, A.R. Johnson, J.A. Janowicz, C.F. Man, D.F. Ortwine, C.F. Purchase, 2nd, A.D. White, D.J. Hupe, A rationalization of the acidic pH dependence for stromelysin-1 (Matrix metalloproteinase-3) catalysis and inhibition, J. Biol. Chem. 275 (2000) 11026-11033.
[33] R.K. Harrison, B. Chang, L. Niedzwiecki, R.L. Stein, Mechanistic studies on the human matrix metalloproteinase stromelysin, Biochemistry 31 (1992) 10757-10762.
[34] J.P.G. Malthouse, ^{13}C NMR of Enzymes, Prog. Nucl. Magn. Reson. Spectrosc. 18 (1986) 1-60.
[35] E. Oldfield, R.S. Norton, A. Allerhand, Studies of Individual Carbon Sites of proteins in Solution by Natural Abundance Carbon 13 Nuclear Magnetic resonance Spectroscopy, J. Biol. Chem. 250 (1975) 6368-6380.
[36] J.P.G. Malthouse, M.D. Finucane, A study of the relaxation parameters of a 13C-enriched methylene carbon and a 13C-enriched perdeuteromethylene carbon attached to chymotrypsin, Biochem. J. 280 (1991) 649-657.
[37] P.A. Frey, S.A. Whitt, J.B. Tobin, A Low-Barrier Hydrogen Bond in the Catalytic Triad of Serine Proteases, Science (New York, N.Y 264 (1994) 1927-1930.
[38] C.M. Holman, C.C. Kan, M.R. Gehring, H.E. Van Wart, Role of His-224 in the anomalous pH dependence of human stromelysin-1, Biochemistry 38 (1999) 677-681.
[39] R.P. Bell, M.H. Rand, K.M.A. Wynne-Jones, Kinetics of the hydration of acetaldehyde, Trans. Faraday Soc. 52 (1956) 1093-1102.

[40] M. Ikejiri, M.M. Bernardo, R.D. Bonfil, M. Toth, M. Chang, R. Fridman, S. Mobashery, Potent mechanism-based inhibitors for matrix metalloproteinases, J. Biol. Chem. 280 (2005) 33992-34002.
[41] Q.Z. Ye, L.L. Johnson, D.J. Hupe, V. Baragi, Purification and characterization of the human stromelysin catalytic domain expressed in Escherichia coli, Biochemistry 31 (1992) 11231-11235.
[42] Q.Z. Ye, L.L. Johnson, I. Nordan, D. Hupe, L. Hupe, A recombinant human stromelysin catalytic domain identifying tryptophan derivatives as human stromelysin inhibitors, J. Med. Chem. 37 (1994) 206-209.

Scheme legends

Scheme 1: Structure of the UK-370106-COOH inhibitor and its glyoxal and hydroxymate derivatives.

Inhibitor	R
UK-370106-COOH	COOH
UK-370106-$CO^{13}CHO$	COCHO
UK-370106-CONHOH	CONHOH

Scheme 2. Structure and Chemical Shifts of Glyoxal Inhibitors. The structures and chemical shifts in (a)-(c) are for the UK-370106-$CO^{13}CHO$ inhibitor, the solvents in which the chemical shifts are measured are in parentheses, the solvents were H_2O containing 20-30% (v/v) d_6-DMSO and DMSO (100% (v/v). The structures and chemical shifts in (d) and (e) are of peptide glyoxals in H_2O containing 10% (v/v) deuterium oxide [1].

Scheme 3. Kinetic Schemes for catalysis and inhibition of metalloproteases. A; Catalysis by most metalloproteases, B; Catalysis and inhibition of SCD by UK-370106-$CO^{13}CHO$.

Figure legends

Fig. 1. Effect of pH on the stability of SCD at 25 ˚C. 12 μM SCD was incubated in 0.25M buffer at 25 ˚C and 10 μl samples were removed at various times and assayed for catalytic activity using the 1 mL thiopeptolide substrate assay containing 0.15 M MES buffer at pH 6.0. The 0.25 M buffers (pH values are in parentheses) used were sodium acetate (4.5 and 5.0), MES (5.5 and 6.0), MOPS (7.0 and 8.0) and glycine (9.0 and 10.0). The lines at pHs 6.0, 7.0, 8.0 and 8.4 are mean values of 93.7 ± 3.2, 100.2 ± 4.5, 101.7 ± 3.2 and 90.9 ± 4.0 respectively. The solid line at pH 5.5 was calculated using the equation y = mx + c and the fitted parameters m = -0.0569 ± 0.0038 and c = 94.1 ± 1.7. The solid lines at pHs 5.0 and 9.0 were calculated using the equation $y = a.e^{-kt}$. The fitted parameters were pH 5.0: k = 0.018 ± 0.002 s^{-1} and a = 98.8 ± 3.7 %, pH 9.0: k = 0.010 ± 0.001 s^{-1} and a = 99.4 ± 2.9%. The solid lines at pHs 4.5 and 10.0 were calculated using the equation $y = a.e^{-k1t} + b.e^{-k2t}$. The fitted parameters were pH 4.5: k_1 = 0.182 ± 0.077 s^{-1} , k_2 = 0.0175 ± 0.0117 s^{-1}, a= 66.0 ± 17.9 % and b = 33.4 ± 17.7%.

Fig. 2. Effect of pH on the disassociation constants for the SCD-inhibitor complexes formed with the UK370106-$CO^{13}CHO$ inhibitor at 25 C. The experimental procedures used to determine the Ki values are described in the "Experimental Procedures". In (a) the continuous line was calculated using the equation $K_{i(obs)} = (K_{i1}[H]^2 + K_{i2}K_{a1}[H] + K_{i3}K_{a1}K_{a2})/([H]^2 + K_{i1}[H] + K_{i1}K_{i2})$ and the fitted parameters K_{i1} = 25.6 ± 50.4 μM, K_{i2} = 0.1 ± 2.9 μM (fixed), K_{i3} = 26.6 ± 2.7 μM, pK_{a1} = 4.41 ± 1.52 and pK_{a2} 7.50 ± 0.21. In (b) the continuous line was calculated using the equation $(1/K_{i(obs)}) = (1/K_i)_{max} / (1 + [H]/K_{a1} + K_{a2}/[H])$ and the fitted parameters pK_{a1} = 6.19 ± 0.43, pK_{a2} = 5.85 ± 0.43 and $(1/K_i)_{max}$ = 6.06 ± 4.76 μM^{-1}.

Fig. 3. ^{13}C-NMR spectra of [1-^{13}C]UK 370106-$CO^{13}CHO$ before and after addition to SCD at pH 7. Acquisition and processing parameters were as described in the "Experimental Procedures". Sample

conditions were (a) 0.332 mL, 0.536 mM SCD, 7.0 mM MOPS, 7.0 mM $CaCl_2$, 35.1 μM $ZnCl_2$, 19.9 % (v/v) d_6-dimethylsulfoxide, 9.9% (v/v) ^2H_2O and pH 6.74, (b) 0.502 mL, 0.348 mM [1-^{13}C]UK 370106-CO^{13}CHO, 49.8 mM MOPS, 8.96 mM $CaCl_2$, 44.8 μM $ZnCl_2$, 20.3 % (v/v) d_6-dimethylsulfoxide, 10.0% (v/v) ^2H_2O and pH 7.03, (c) 0.332 mL, 0.528 mM SCD, 0.543 mM [1-^{13}C]UK 370106-CO^{13}CHO, 22.0 mM MOPS, 6.9 mM $CaCl_2$, 34.6 μM $ZnCl_2$, 20.5 % (v/v) d_6-dimethylsulfoxide, 9.8% (v/v) ^2H_2O and pH 7.00, (d) 342 mL, 0.520 mM SCD, 0.535 mM [1-^{13}C]UK 370106-CO^{13}CHO,).527 mM UK370106-COOH, 21.7 mM MOPS, 6.8 mM $CaCl_2$, 34.0 μM $ZnCl_2$, 21.7 % (v/v) d_6-dimethylsulfoxide, 9.6% (v/v) ^2H_2O and pH 7.02. Samples (a), (c) and (d) were in 5mm Shigemi tubes. Sample (b) was in a conventional 5mm NMR tube.

Fig. 4. The effect of pH on the ^{13}C-NMR spectra of [1-^{13}C]UK 370106-CO^{13}CHO bound to SCD. Acquisition and processing parameters were as described in the "Experimental Procedures". Sample (d) at pH 7.06 had a volume of 0.332 mL and it contained 0.795 mM SCD, 0.923 mM [1-^{13}C]UK 370106-CO^{13}CHO, 13.8 mM MOPS, 6.9 mM $CaCl_2$, 34.4 μM $ZnCl_2$, 10% (v/v) ^2H_2O and 21% (v/v) d_6-dimethyl sulfoxide. Samples (c) and (b) with pH values of 6.52 and 6.01 were obtained by adding 7.5 and 17.0 μl of 1M MES pH 5.7 respectively to sample (d). Sample (a) at pH 5.52 was formed by adding 7μl of 1M sodium acetate buffer pH 4.44 to sample (b). Sample (e) at pH 7.54 had a volume of 0.330 mL and it contained 0.67 mM SCD, 0.929 mM [1-^{13}C]UK 370106-CO^{13}CHO, 14.2 mM MOPS, 6.1 mM HEPES, 7.1 mM $CaCl_2$, 35.5 μM $ZnCl_2$, 10% (v/v) ^2H_2O and 21% (v/v) d_6-dimethyl sulfoxide. Samples (f) and (g) with pH values of 7.96 and 8.44 respectively were obtained by adding 4.0 and 16.0 μl respectively of 1M HEPES pH 8.4 to sample (e).

Fig. 5. Effect of pH on the intensity of the ^{13}C NMR signal at 92 ppm from [1-^{13}C]UK 370106-CO^{13}CHO bound to SCD. Acquisition and processing parameters were as described in the "Experimental Procedures". Sample conditions are the same as in Fig. 4. The continuous line was

calculated using the equation $I_{i(obs)} = I_{max} / (1 + [H]/K_{a1} + K_{a2}/[H])$ and the fitted parameters pK_{a1} = 5.75 ± 0.22, pK_{a2} = 7.78 ± 0.20 and I_{max} = 125 ± 19%.

Fig. 6. The effect of pH on the ^{1}H-NMR spectra of the hydrogen bonded protons of SCD and of its complexes with the inhibitors UK370106-COOH and UK370106-CO^{13}CHO. Acquisition and processing parameters were as described in the "Experimental Procedures". (A) SCD. Sample conditions were (1) pH 5.99, 0.3325 µl, 0.89 mM SCD, 10% (v/v) $^{2}H_2O$, 20% (v/v) d_6-dimethyl sulfoxide, 6.9 mM MOPS, 6.9 mM $CaCl_2$, 7.5 mM sodium acetate and 0.035 mM $ZnCl_2$. 1.5,1.5,1.5,4.0 and 14.0 µl of 1M HEPES buffer, pH 8.6 was added to samples 2, 3, 4, 5 and 6 respectively to change the pH as indicated in Fig. 5A. (B) SCD and UK370106-COOH. Sample conditions were (1) pH 6.05, 0.345 µl, 0.80 mM SCD, 0.91 mM UK370106-COOH, 9.6% (v/v) $^{2}H_2O$, 21.7% (v/v) d_6-dimethyl sulfoxide, 12.5 mM MOPS, 6.7 mM $CaCl_2$, 11.6 mM sodium acetate and 0.033 mM $ZnCl_2$. To change the pH as indicated in Fig. 5B, 2.5, 3.0, 4.0,10.0 and 15.0 µl of 1M HEPES buffer, pH 8.6 were added to samples 2, 3, 4, 5 and 6 respectively. (C) SCD and UK370106-CO^{13}CHO. Sample conditions were (1) pH 6.02, 0.3715 µl, 0.79 mM SCD, 0.74 mM UK370106-CO^{13}CHO, 8.9% (v/v) $^{2}H_2O$, 17.8% (v/v) d_6-dimethyl sulfoxide, 6.2 mM MOPS, 6.2 mM $CaCl_2$, 39 mM sodium acetate, 60.4 mM HEPES and 0.031 mM $ZnCl_2$. To change the pH as indicated in Fig. 5C, 4.5, 2.0, 2.6 and 2.0 µl of 1M HEPES buffer, pH 8.6 were added to samples 2, 3, 4 and 5 respectively. Also 10 and 40 µl of 1M glycine at pH 9.8 were added to samples 5 and 6 respectively.

Table 1

Table 1: Catalytic parameters for the stromelysin catalysed hydrolysis of the thiopeptolide substrate Acetyl-Proline-Leucine-Glycine-[2-mercapto-4-methyl-pentanoyl]-Leucine-Glycine-OC_2H_5

Stromelysin	pH	C	Ki (uM)	Reference
Phe^{83} to Gly^{247}	6.0	25	395	Present work
Phe^{83} toThr^{255}	6.0	22	270	[41]
Phe^{83} toThr^{255}	6.0	22	469	[42]
Full length	6.0	22	518	[42]

Table 2

Table 2
Disassociation constants for stromelysin-1 inhibitors

Inhibitor	pH	C	K_i (nM)	Reference
UK-370106-CONHOH	7.50	37	2.0[a]	[18]
UK-370106-COOH	7.50	37	21.4[b]	[18]
UK-370106-CO^{13}CHO	7.56	37	10,700	Present work
UK-370106-CO^{13}CHO	7.56	25	18800	Present work

a: estimated from an IC_{50} value of 2.1 nM [18].

b: estimated from an IC_{50} value of 23 nM [18].

Table 3

Table 3
pK_a values determined at 25 ˚C from pH dependent changes in the intensities of the NMR signals from 11.0 to 14.0 ppm.

Compound	ppm of observed signal		
	12.9	13.1	13.5
		pK_a values[a]	
SCD	8.01±0.16	6.79±0.06	7.50± 0.09
SCD-UKCOOH		7.11±0.09	7.32±0.09
SCD-UKCO^{13}CHO		7.07 ±0.10	7.02 ±0.12

[a] The pK_a values were obtained by fitting intensities of the appropriate signals at the pH values given in Fig. 5 to the equation $I_{obs}=I_{max}/(1+K_a/[H])$.

Fig1

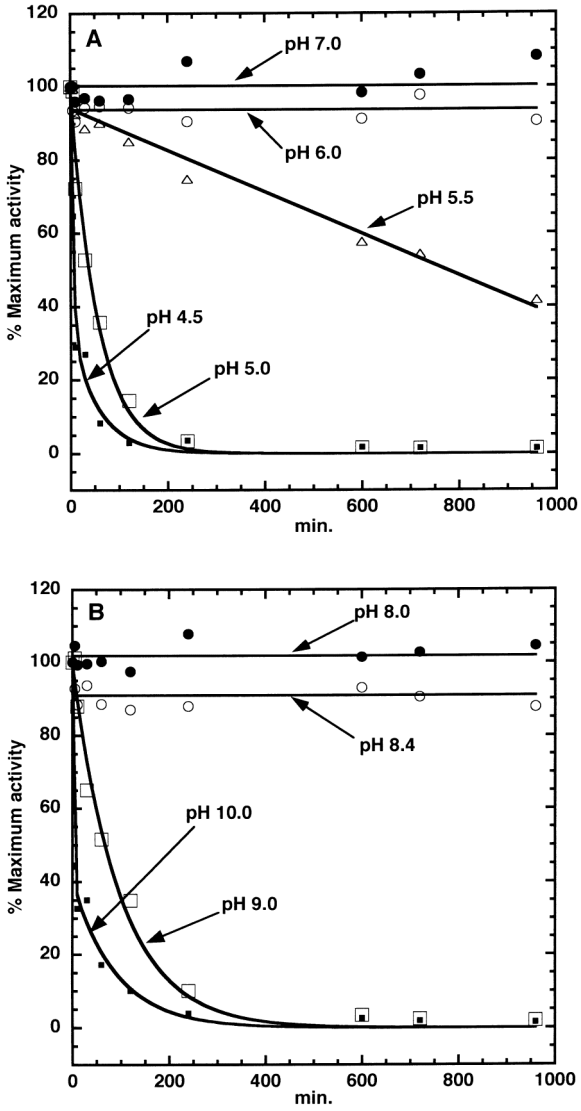
A
pH 7.0
pH 6.0
pH 5.5
pH 4.5
pH 5.0
% Maximum activity
min.
B
pH 8.0
pH 8.4
pH 10.0
pH 9.0
% Maximum activity
min.

Fig2

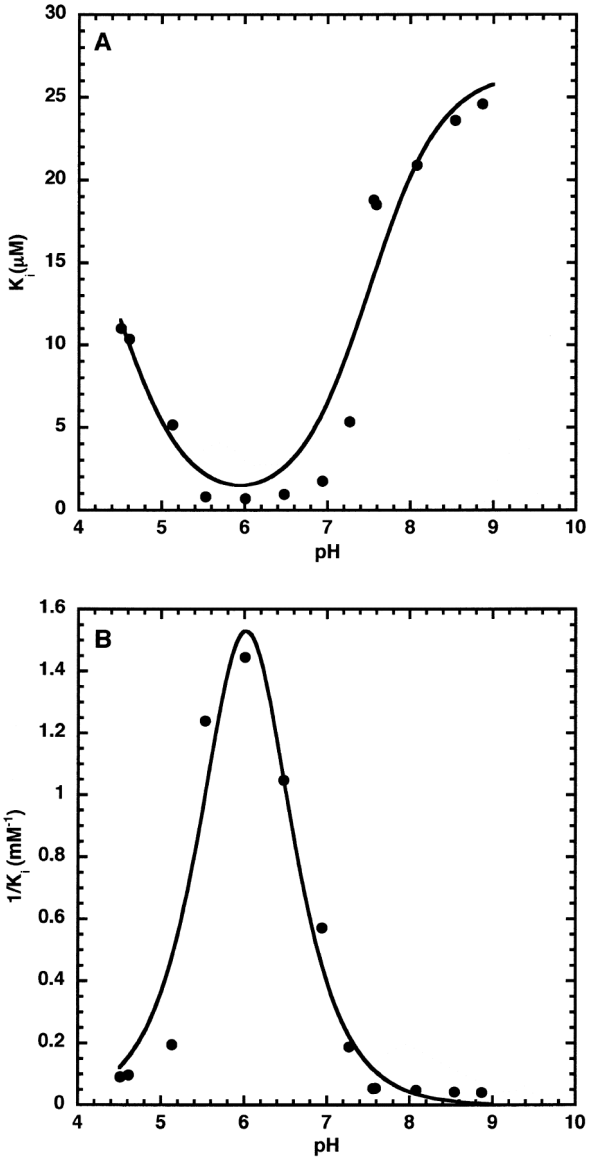

Fig3

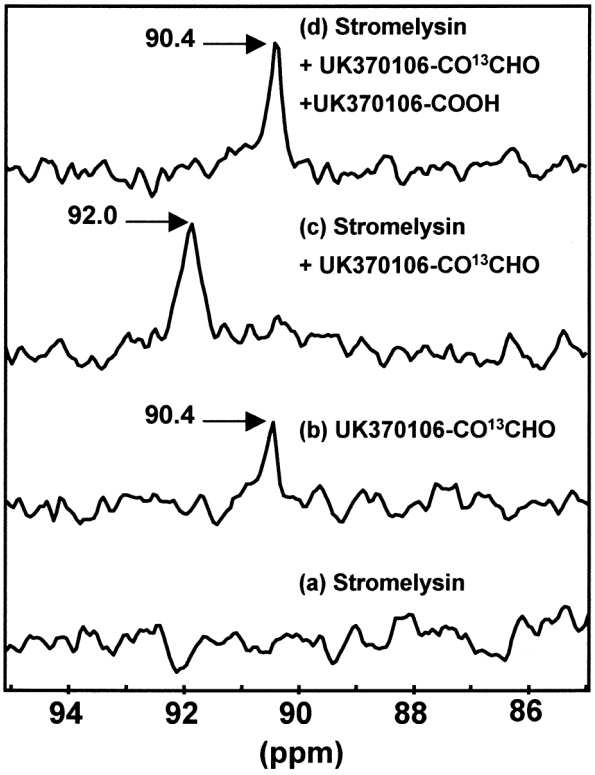
90.4
(d) Stromelysin
+ UK370106-CO13CHO
+UK370106-COOH
92.0
(c) Stromelysin
+ UK370106-CO13CHO
90.4
(b) UK370106-CO13CHO
(a) Stromelysin
94
92
90
88
86
(ppm)

Fig4

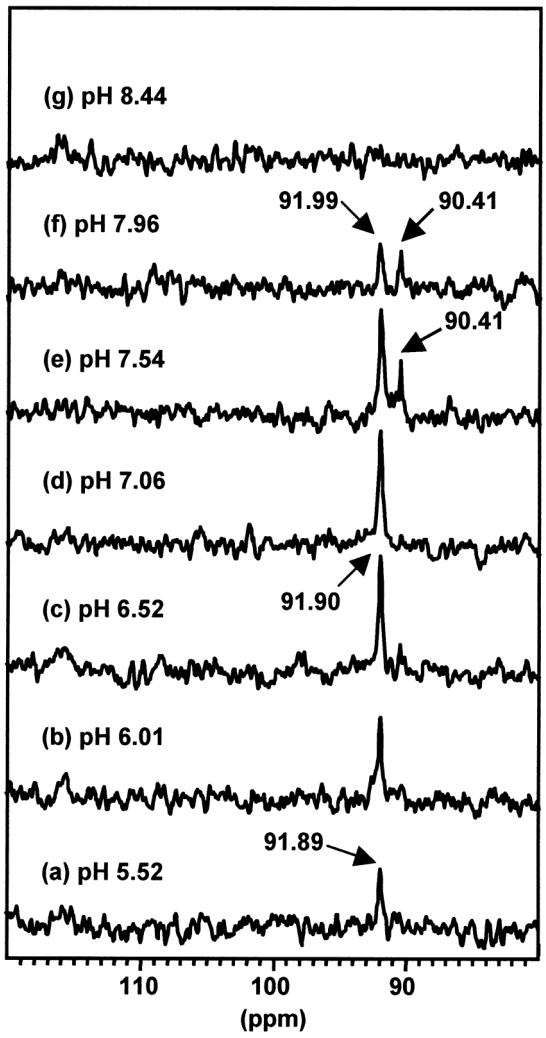
(g) pH 8.44
91.99
90.41
(f) pH 7.96
90.41
(e) pH 7.54
(d) pH 7.06
91.90
(c) pH 6.52
(b) pH 6.01
91.89
(a) pH 5.52
110
100
90
(ppm)

Fig5

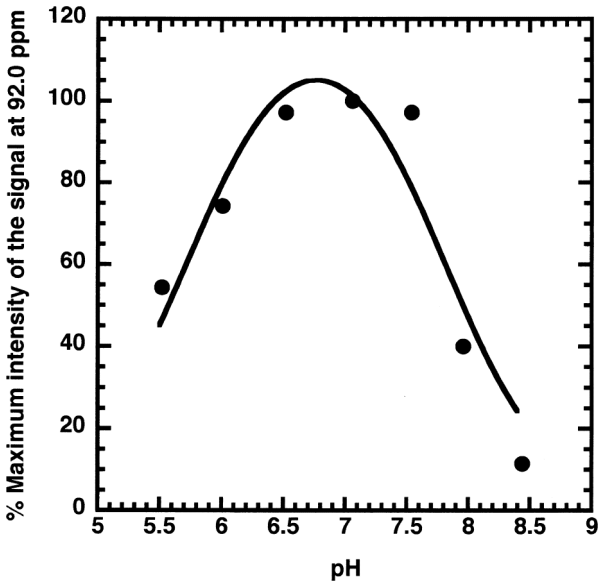
% Maximum intensity of the signal at 92.0 ppm
120
100
80
60
40
20
0
5
5.5
6
6.5
7
7.5
8
8.5
9
pH

Fig6

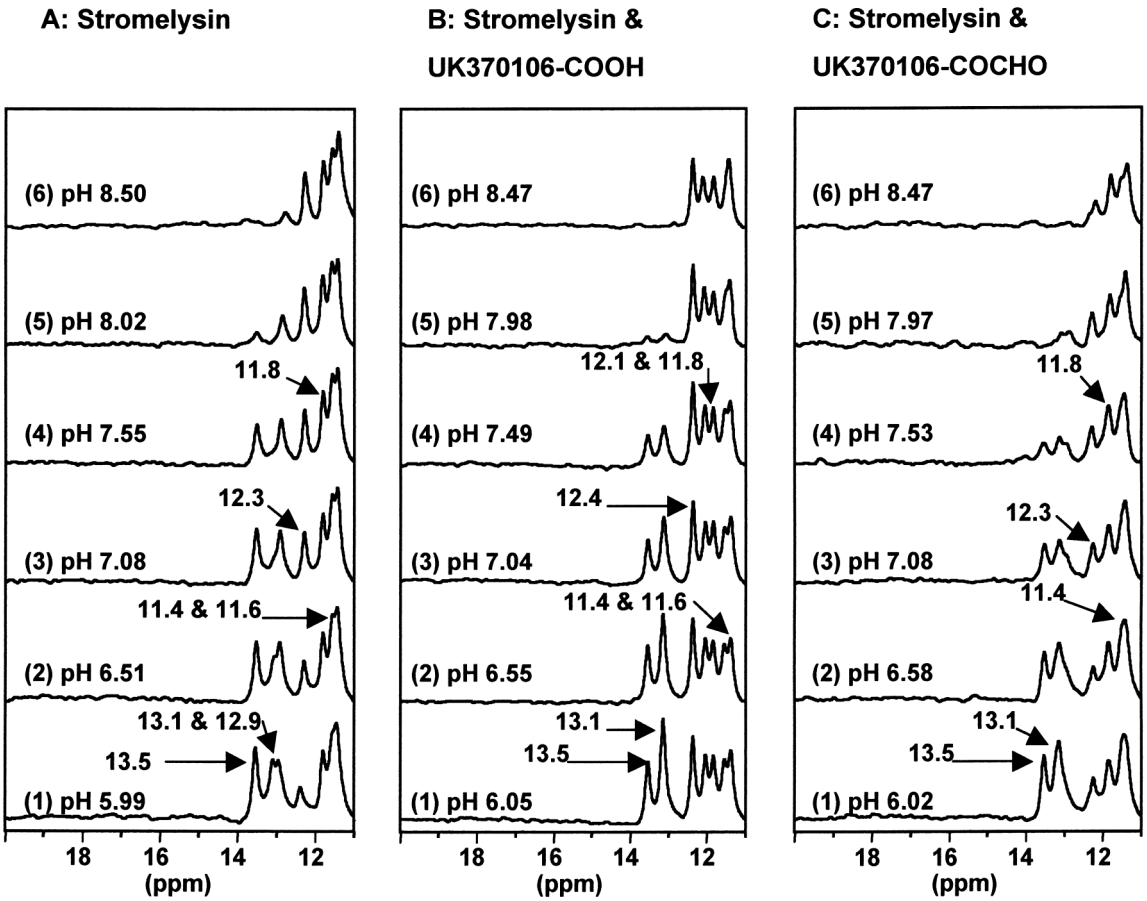
A: Stromelysin
B: Stromelysin &
UK370106-COOH
C: Stromelysin &
UK370106-COCHO
(6) pH 8.50
(5) pH 8.02
11.8
(4) pH 7.55
12.3
(3) pH 7.08
11.4 & 11.6
(2) pH 6.51
13.1 & 12.9
13.5
(1) pH 5.99
18
16
14
12
(ppm)
(6) pH 8.47
(5) pH 7.98
12.1 & 11.8
(4) pH 7.49
12.4
(3) pH 7.04
11.4 & 11.6
(2) pH 6.55
13.1
13.5
(1) pH 6.05
18
16
14
12
(ppm)
(6) pH 8.47
(5) pH 7.97
11.8
(4) pH 7.53
12.3
(3) pH 7.08
11.4
(2) pH 6.58
13.1
13.5
(1) pH 6.02
18
16
14
12
(ppm)

Scheme1

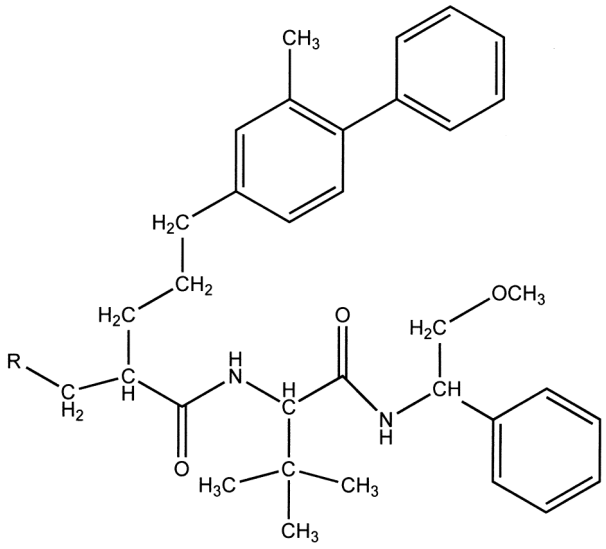

Scheme2

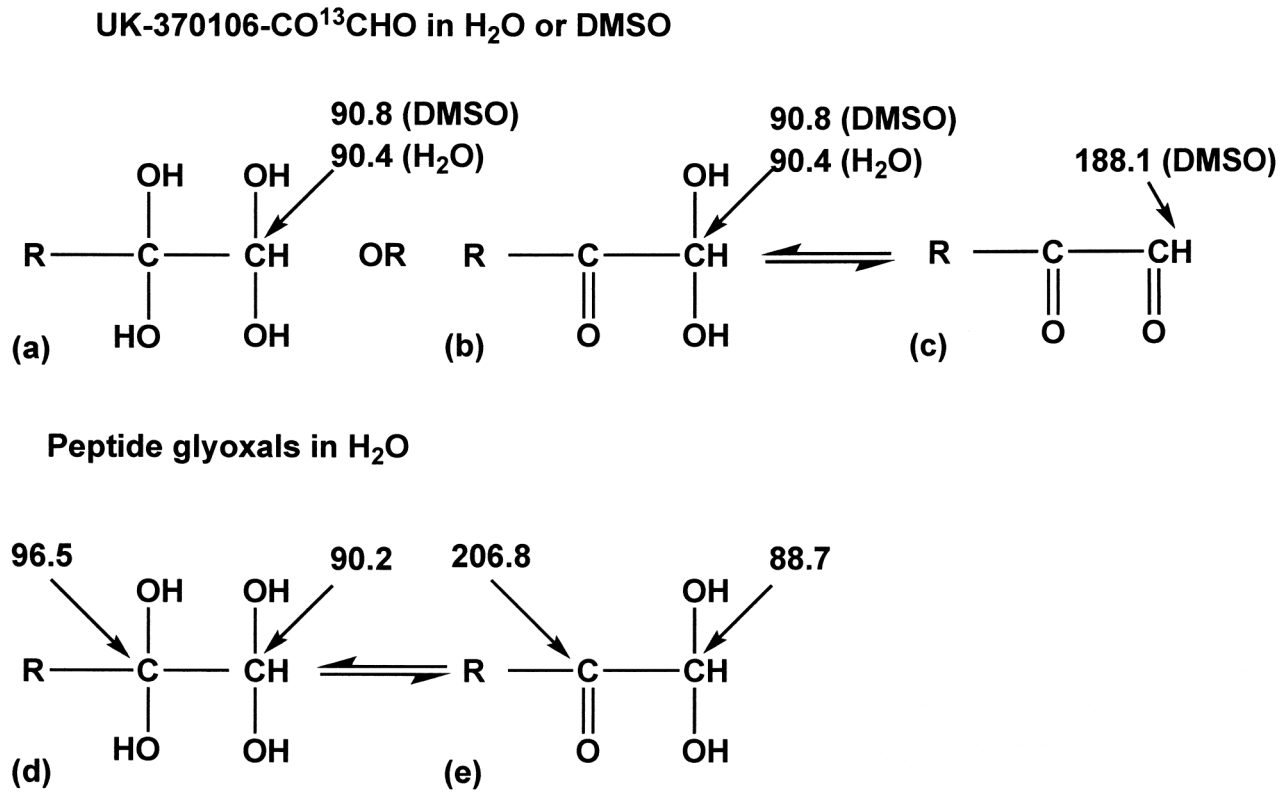
UK-370106-CO13CHO in H2O or DMSO
90.8 (DMSO)
90.4 (H2O)
OH
OH
R
C
CH
OR
HO
OH
(a)
90.8 (DMSO)
90.4 (H2O)
OH
R
C
CH
O
OH
(b)
188.1 (DMSO)
R
C
CH
O
O
(c)
Peptide glyoxals in H2O
96.5
90.2
206.8
88.7
OH
OH
R
C
CH
HO
OH
(d)
R
C
CH
O
OH
(e)

Scheme3

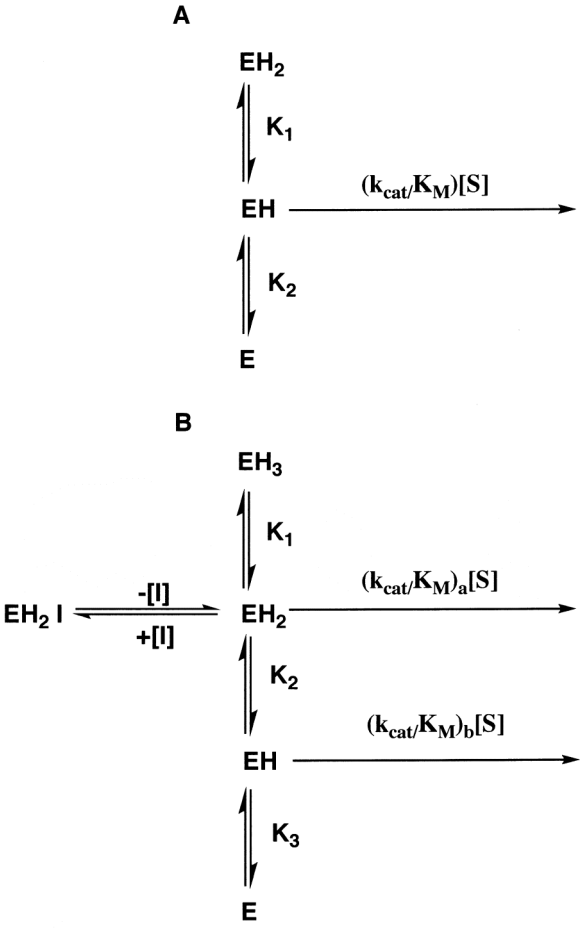
A
EH2
K1
(kcat/KM)[S]
EH
K2
E
B
EH3
K1
(kcat/KM)a[S]
EH2 I
-[I]
+[I]
EH2
K2
(kcat/KM)b[S]
EH
K3
E